SCANNING VOL. 38, 297–302 (2016)

Optical and Surface Properties of the In Doped GaAs Layer Deposition Using Thermionic Vacuum Arc Method

Suat Pat,[1] Soner Özen,[1] Volkan Şenay,[2] Şadan Korkmaz,[1] and Veli Şimşek[3]

[1]Department of Physics, Eskişehir Osmangazi University, Turkey
[2]Primary Science Education Department, Bayburt University, Turkey
[3]Central Research Laboratory of Bilecik Şeyh Edebali University, Bilecik, Turkey

Summary: A broadband optical transparent InGaAs semiconductor layer production of micron thicknesses was produced in only 75 s by thermionic vacuum arc (TVA) method at the first time. The optical and surface properties of the produced layers have been investigated. InGaAs structure is using in electronics and optoelectronics devices. The main advantage of TVA method is its fast deposition rate, without any loss in the quality of the films. Doping is a very simple and fast according to common production methods. InGaAs is an alloy of indium arsenide (InAs) and gallium arsenide (GaAs). InAs with (220) crystallographic direction and GaAs with (024)/(022) crystallographic directions were detected using by XRD analysis. GaAs and InAs are in the cubic and zinc blende crystal system, respectively. According to the transmittance spectra, sample has a broadband transparency in the range of 1000–3300 nm. According to results, defined TVA method for In doping to GaAs is proper fast and friendly method. SCANNING 38:297–302, 2016. © 2015 Wiley Periodicals, Inc.

Key words: InGaAs, III/V doped semiconductor, TVA, optical properties

Introduction

Gallium arsenide (GaAs) and doped GaAs are widely used semiconductor compounds used in some diodes, photovoltaic, opto-electronic device, field-effect transistors (FETs), fiber optic communication, solar cell, infra red detectors, and lasers (Levine, '93; Devaux *et al.*, '95; Raisky *et al.*, '98; Metzger *et al.*, 2001; Choi *et al.*, 2005). Many applications, GaAs structures are doped with trace impurity elements. Doping of semiconductors is the process of locally manipulating their charge carrier density and conductivity. This is a key technology for semiconductor-based electronic devices (Norman *et al.*, 2005; Chen *et al.*, 2009; Oswald *et al.*, 2010).

Conventional doping is usually achieved via the bombardment of semiconductors with energetic ions (the dopants) followed by thermal annealing; this is referred to as ion implantation. General chemical formula of III/V doped semiconductor is given as $In_xGa_{1-x}As$. x ratio was calculated as 0.12 in this paper. Obtained general formula of produced layers is $In_{0.12}Ga_{0.88}As$ (Guha *et al.*, '90; Chin and Lin, '96, Schapers *et al.*, '98; Mukai and Sugawara, '99; Parker *et al.*, '99; Metzger *et al.*, 2001; Dal Savio *et al.*, 2006). We report a new growth method for InGaAs. The generated plasma was produced together with doping element (In) and GaAs material. X-Ray Diffraction (XRD) characterization, field emission scanning electron microscopy (FESEM), energy dispersive X-ray spectroscopy (EDX), atomic force microscopy (AFM), UV-Vis-NIR spectrophotometry, optical tensiometry and an interferometry measurement systems and tools were used for the identification of the produced InGaAs sample.

Experimental

A thermionic vacuum arc (TVA) technique was used for the first time production of $In_xGa_{1-x}As$ thin films. TVA is an anodic plasma generator and thin films can also produce. (Okur *et al.*, 2007; Ekem *et al.*, 2008; Balbag and Pat, 2011; Pat *et al.*, 2013, 2014a,b). InGaAs thin film layers were coated on glass substrates. A schematic drawing of the TVA method is shown in Figure 1 (Pat et al., 2013). We present a new deposition

Contract grant sponsor: ESOGU BAP commission; Contract grant number: 201519D06.

Address for reprints: Suat Pat, Department of Physics, Eskiehir Osmangazi University, Meelik Campus 26480, Turkey.
E-mail: suatpat@ogu.edu.tr

Received 10 June 2015; Accepted with revision 1 September 2015

DOI: 10.1002/sca.21269
Published online 11 September 2015 in Wiley Online Library (wileyonlinelibrary.com).

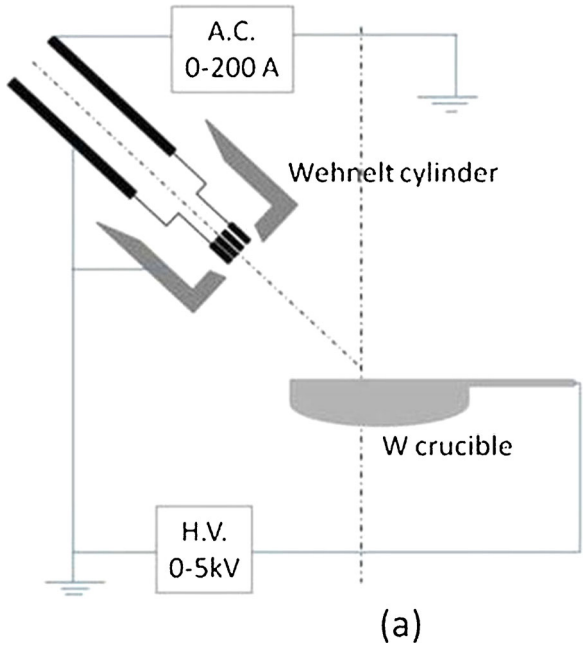

Fig 1. Schematically view of the TVA electrode arrangement [20].

method in a very short production time of 75 s for InGaAs thin film. High-purity GaAs (0.25 g) and In (0.05 g) were used as the anode material. The parameters of TVA are the filament current (18 A), applied voltage (500 V), working pressure (4.10^{-5} Torr), deposition time (75 s) and discharge current (approximately 0.5 A). All production and measurements were realized at room temperature.

Results and Discussion

InGaAs is an alloy of gallium arsenide and indium arsenide. Chemically formula is given as $In_xGa_{1-x}As$. The properties of InGaAs can be varied by changing the ratio of In amount (Guha *et al*., '90; Chin and Lin, '96; Schapers *et al.*, '98; Parker *et al*., '99; Metzger *et al*., 2001; Dal Savio *et al.*, 2006). The thickness of the produced In doped GaAs layers, InGaAs, were measured as approximately 2 μm. Thickness of the deposited layer was measured using Filmetric F20 tool. Thickness of the film calculates by reflection measurement of the deposited layer. Cauchy model is used for the determination of the thickness.

PANalytical Empyrean XRD was used to determine of the microstructure and crystallographic data. XRD spectra were recorded in the 2-Theta range between 20° and 90° using CuKα radiation at 40 mA and 40 kV ($\lambda = 1.5406$ A). Film dimensions were 1×1 cm. XRD spectra of In doped GaAs layer is given in Figure 2. All samples were grown on glass substrates. All peaks were assigned in Figure 2. Crystal direction was found to be (022) plane and (024) plane for the InGaAs/glass

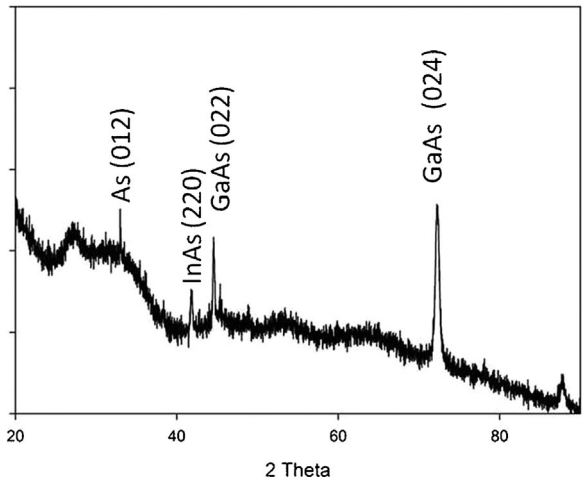

Fig 2. XRD spectra of deposited InGaAs.

sample at 45.322° and 75.060°. Other peaks at approximately located at 42° and 33° corresponds to (220) plane for InAs (Wells *et al*., '95) and (012) plane for As. Some crystallographic data are summarized in Table I. According to XRD data, produced InGaAs alloys have two crystal phases. These are GaAs (card number: 98-060-0516), As (card number:98-001-6517), and InAs.

After a critical thickness of the thin film phase increases with the film thickness. The critical film thickness is affecting the substrates temperatures (Bouchoms *et al.*, '99).

A scanning electron microscope with a field emission cathode (Zeiss Supra 40VP) was used for surface imaging analyses. Field emission scanning electron microscope images are shown in Figure 3. As can be seen in Figure 3, two type spherical structures have been observed. These types are similar to each other. These structures are called small sphere and big sphere. Big sphere structures are formed from small spheres. Small sphere diameter is approximately 30–40 nm.

Supra V40 was used for the EDX analyses. The elemental analysis results are shown in Table II. Obtained EDX spectrum is shown in Figure 4. Chemically formula of deposited material is given as $In_xGa_{1-x}As$. x value calculated as 0.10. This ratio calculated from EDX analysis results. This ratio is the most common value for the presented papers about In doped

TABLE I Crystallographic information obtained from XRD spectra

	InAs (taken from ref. 21)	GaAs	As
(hkl)	(220)	(022)/(024)	(012)
Crystal system	Zinc blende	Cubic	Hexagonal
d space (A)	2.14	1.99/1.26	2.76

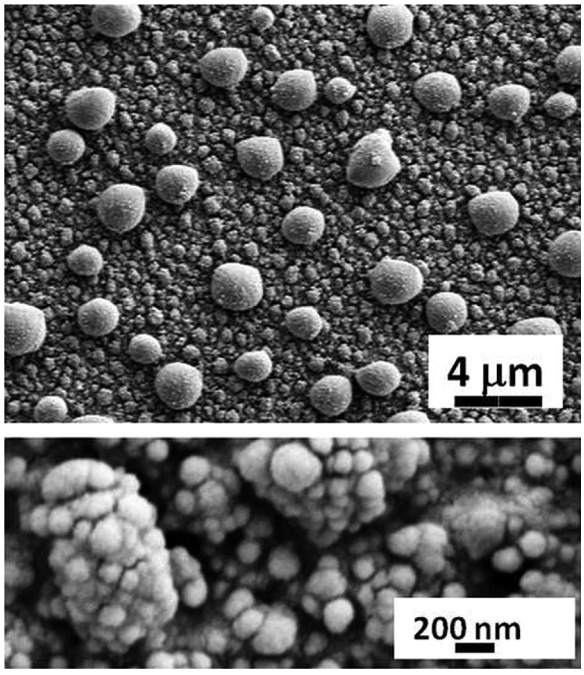

Fig 3. FESEM images of deposited InGaAs.

TABLE II EDX analysis results

Element	Weight ratio (%)	Atomic ratio (%)
Gallium	65	70
Arsenic	20	20
Indium	15	10

GaAs structures (Wells *et al.*, '95; Chin and Lin, '96; Guzelian *et al.*, '96; Parker *et al.*, '99; Zhuang *et al.*, 2000; Metzger *et al.*, 2001; Dal Savio *et al.*, 2006; Oswald *et al.*, 2010).

Ambios Q-Scope AFM was used to determine surface morphology and surface roughness. AFM measurements were realized at room temperatures. Cantilever is NSC16. Resonance frequency was found at 185.8 kHz. Force constant of the cantilever is 42 N/m. Non-contact mode was used for all AFM measurements. Operating software is AFM Q-Scope. Auto engaging mode of software was used. 2D and 3D AFM images are shown in Figures 5. The AFM images were obtained using a $4000 \times 4000\,nm^2$ scale. The average surface roughness (RMS) was calculated as 26 nm for from the seven parallel lines of the surface by AFM Q-scope operating software. This value for the InGaAs can be obtained using traditional deposition methods such as MBE and MOCVD. Obtained images are similar to FESEM images.

Optical absorption and transmission measurements have been carried out using Shimadzu Solid Spec-3700 DUV Spectrophotometer covering the spectral range from 190 to 3300 nm. Absorption values are relatively high. Especially, produced materials are completely absorbed the UV-Vis region. An absorbance spectrum of the sample is shown in Figure 6(a). InGaAs detector has highly transmittance the light for the wavelength range 800–1800 nm. But, the structural properties of the InGaAs can affect the transmission

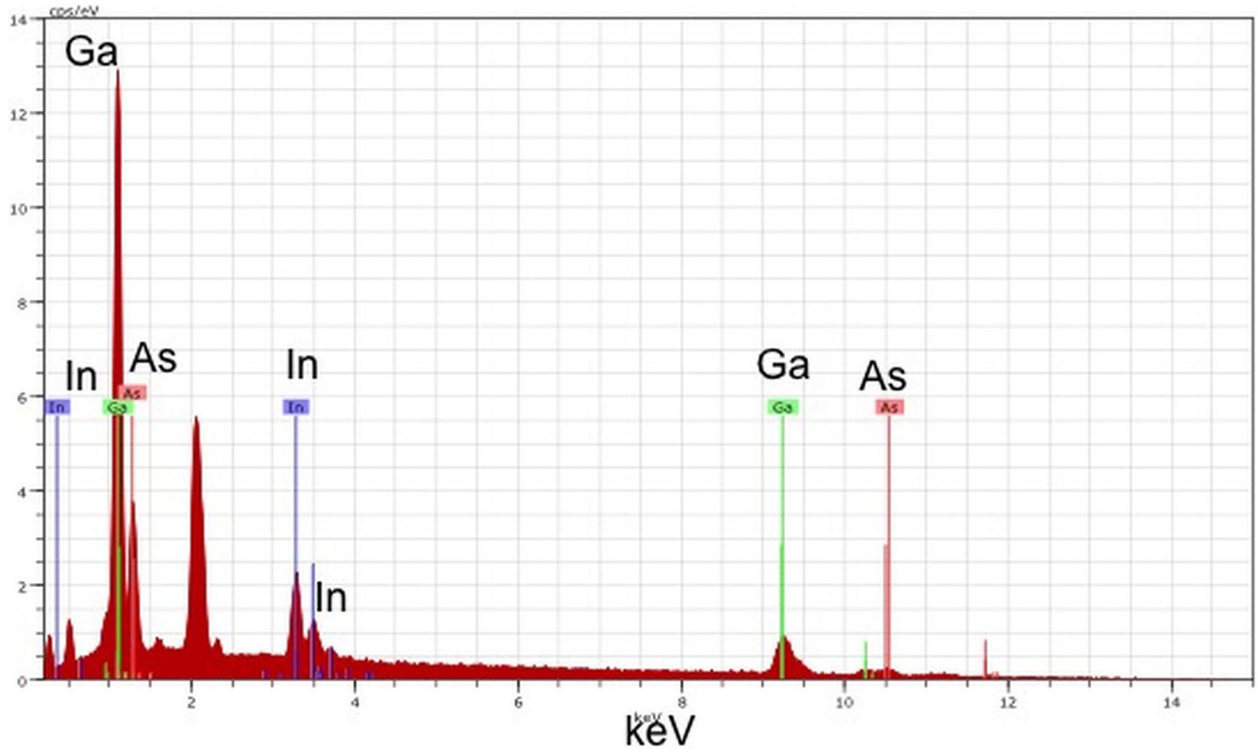

Fig 4. EDX spectra of deposited InGaAs.

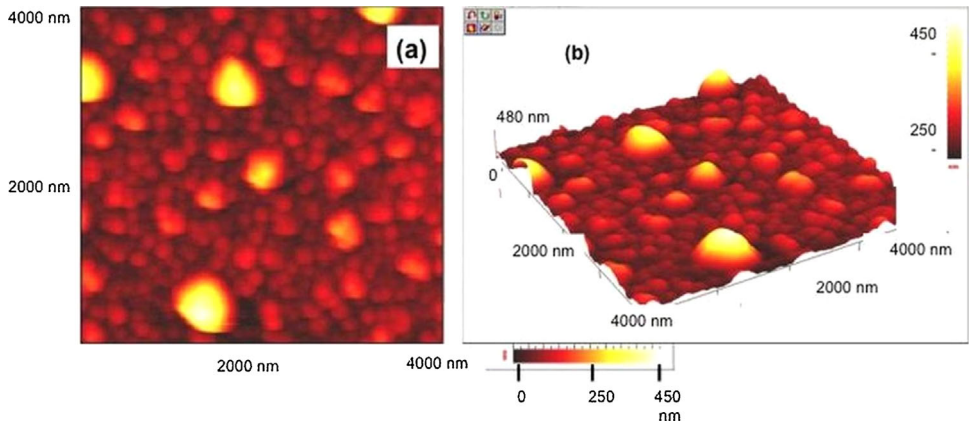

Fig 5. 2D and 3d AFM images of InGaAs.

range. These values can shift to upper wavelengths based on structural properties. As can be seen in Figure 6(b), deposited InGaAs layer absorbs wavelengths below approximately 1000 nm. Up to 3300 nm, obtained layers are relatively transparent. Transparency decreases with the increasing film thickness. Film thickness is increase with the deposition process time in TVA. Also, thickness of the film depends on the growth rate and morphology (Taguchi *et al*., 2002). Broadband optical transparent

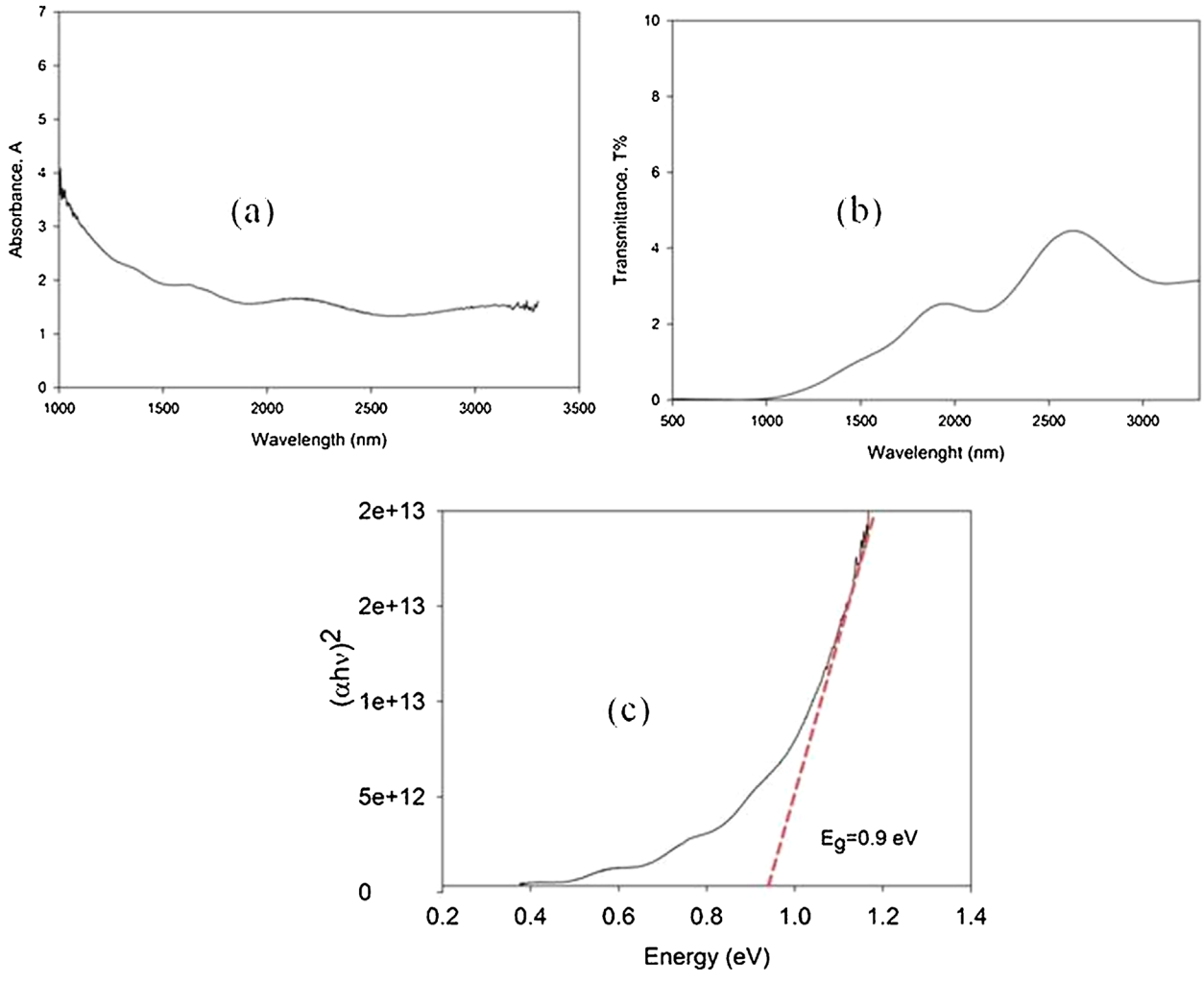

Fig 6. Transmittance and absorbance spectra.

InGaAs layers of micron thicknesses have been achieved. Production duration is only 75 s.

A $(\alpha h\nu)^2$-eV plot was used for the band gap calculations. The plot is shown in Figure 6(c). According to this plot, band gaps of 0.47, 0.60, and 1.00 eV were determined. Band gap of the un-doped GaAs is approximately 1.45 eV (Pat *et al.*, 2015). Doping impurities and rates strongly affects this value. This is concluded that GaAs compound are linked to another element, because band gap values are decreased to lower value. The band gap of the InAs structure is giving between 1.05 and 1.15 eV (Guzelian *et al.*, '96). x value for $In_xGa_{1-x}As$ are strongly effect ban gap values of the structure. Also, doping concentration or defect distribution can affect the all properties (Marchewka *et al.*, 2014). The band gap energy of the $In_xGa_{1-x}As$ varies between 0.50 eV and 1.00 eV. x value is varied between 0.07 and 0.77 (Schapers *et al.*, '98; Parker *et al.*, '99; Zhuang *et al.*, 2000; Metzger *et al.*, 2001; Pat *et al.*, 2015). Obtained band gap values are very close to literatures values.

The surface free energies were calculated from the contact angle measured by an Attension Theta Lite tensiometer. Water, ethylene glycol, di-iodomethane, and formamide liquids were used as a heavy phase for *surface free energy* (SFE) measurements. The SFE of the solid is proportional to the surface tension. SFE is the proportion of surface tension for the solids. The method used and the results obtained are shown in Table III. The minimum value of the measured contact angle (CA) was measured as over 105° for water. It shows that layers are hydrophobic. The SFEs of the films are calculated by various methods. These measurements results were summarized in Table III. Photo image of the used liquid droplets for the SFE determination are illustrated in Figure 7.

TABLE III CA and SFE values

	CA (°)	Method	SFE (mJ/m^2)
Water	105	Acid-Base	29
Formamide	97	Equation of state	23
Ethylene glycol	81	OWRK/Fowkes	31
Di-iodomethane	45	Wu	33
		Zisman	25

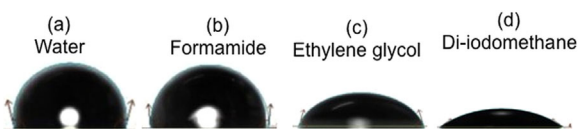

Fig 7. Photo image of the used liquid droplets.

Conclusion

In this paper, a new broadband optical transparent InGaAs layer production of micron thicknesses was produced in only 75 s. The properties of the produced layers have been investigated. InGaAs is an alloy of indium arsenide and gallium arsenide. In content, x is the most important properties for the properties of the $In_xGa_{1-x}As$. InAs with (220) crystallographic direction and GaAs with (024)/(022) crystallographic directions were detected using xrd tool. GaAs and InAs are in the cubic and zinc blende crystal system, respectively. Good surface morphologies and optical properties using by TVA method were obtained. According to the transmittance spectra, sample has a broadband transparency in the range of 1000–3300 nm. Band gap energy is strongly influenced with doping impurities. 1.45 eV transition cannot detect in obtained layer. x value for $In_xGa_{1-x}As$ is strongly effect the band gap values and surface properties of the sample. The band gap energy of the $In_xGa_{1-x}As$ varies between 0.50 eV and 1.00 eV. Obtained band gap value is 0.9 eV and this is very close to literatures values. According to results, introduced In doped method is a proper and friendly method for mass and experimental producing method.

References

Balbag MZ, Pat S. 2011. Electrically conductive and optically transparent polyethylene terephthalate films coated with gold and silver by thermionic vacuum arc. J Plast Film Sheet 27:209–222.

Bouchoms IPM, Schoonveld WA, Vrijmowth J, Klapwijk TM. 1999. Morphology identification of the thin film phases of vacuum evaporated pentaceneonSIO2 substrates. Synthetic Metals 104:175.

Chen W, Qi DC, Gao XY, Wee ATS. 2009. Surface transfer doping of semiconductors. Prog Surf Sci 84:279–321.

Chin A, Lin BC. 1996. High optical quality of strained (111)B In0.12Ga0.88As/GaAs and In0.12Ga0.88As/Al0.2Ga0.8As multiple quantum wells. Appl Phys Lett 68:2717–2719.

Choi WJ, Song JD, Hwang SH, et al. 2005. Low-frequency noise characteristics of InGaAs quantum-dot infrared photodetector structures grown by atomic layer molecular-beam epitaxy. Physica E-Low-Dimensional Systems & Nanostructures 26:366–371.

Dal Savio C, Pierz K, Ade G, et al. 2006. Optical study of single InAs on In0.12Ga0.88As self-assembled quantum dots: biexciton binding energy dependence on the dots size. Appl Phys B-Lasers O 84:317–322.

Devaux F, Chelles S, Ougazzaden A, Mircea A, Harmand JC. 1995. Electroabsorption modulators for high-bit-rate optical communications—comparison of strained Ingaas/Inalas and Ingaasp/Ingaasp. Semicond Sci Tech 10:887–901.

Ekem N, Korkmaz S, Pat S, et al. 2008. ZnO thin film preparation using RF sputtering at various oxygen contents. J Optoelectron Adv Mater 10:3279–3282.

Guha S, Madhukar A, Rajkumar KC. 1990. Onset of incoherency and defect introduction in the initial-stages of molecular-beam epitaxial-growth of highly strained Inxga1-Xas on Gaas(100). Appl Phys Lett 57:2110–2112.

Guzelian AA, Banin U, Kadavanich AV, Peng X, Alivisatos AP. 1996. Colloidal chemical synthesis and characterization of InAs nanocrystal quantum dots. Appl Phys Lett 69:1432–1434.

Levine BF. 1993. Quantum-well infrared photodetectors. J Appl Phys 74:R1–R81.

Marchewka A, Cooper D, Lenser C, et al. 2014. Determination of the electrostatic potential distribution in Pt/Fe:SrTiO3/Nb:SrTiO3 thin-film structures by electron holography. Sci Rep 4:6975.

Metzger WK, Wanlass MW, Ellingson RJ, Ahrenkiel RK, Carapella JJ. 2001. Auger recombination in low-band-gap n-type InGaAs. Appl Phys Lett 79:3272–3274.

Mukai K, Sugawara M. 1999. Suppression of temperature sensitivity of interband emission energy in 1.3-mu m-region by an InGaAs overgrowth on self-assembled InGaAs GaAs quantum dots. Appl Phys Lett 74:3963–3965.

Norman AG, Hanna MC, Dippo P, et al. 2005. InGaAs/GaAs QD superlattices: MOVPE growth, structural and optical characterization, and application in intermediate-band solar cells. Conference Record of the Thirty-First IEEE Photovoltaic Specialists Conference - 2005 43–48.

Okur S, Kalkanci M, Pat S, et al. 2007. MgB2 superconducting thin films sequentially fabricated using DC magnetron sputtering and thermionic vacuum arc method. Physica C: Superconductivity 466:205–208.

Oswald J, Hazdra P, Kuldova K, et al. 2010. Electro- and photoluminescence of InAs/GaAs quantum dot structures. Quantum Dots 245.

Pat S, Balbag MZ, Korkmaz S. 2014a. Mechanical properties of deposited carbon thin films on sapphire substrates using atomic force microscopy (AFM). Ceram Int 40:10159–10162.

Pat S, Balbag MZ, Korkmaz S. 2013. Ultra thin carbon films deposited on SrTiO3 substrates by thermionic vacuum arc. Nano 8.

Pat S, Korkmaz S, Balbag MZ. 2014b. A new deposition technique using reactive thermionic vacuum arc for ZnO thin film production. J Nanoelectron Optoe 9:437–441.

Pat S, Korkmaz Ş, Özen S, Şenay V. 2015. Direct and fast growth of GaAs thin films on glass and polyethylene terephthalate substrates using a thermionic vacuum arc. J Mater Sci: Mater Electron 26(4):2210–2214.

Parker CA, Roberts JC, Bedair SM, et al. 1999. Determination of the critical layer thickness in the InGaN/GaN heterostructures. Appl Phys Lett 75:2776–2778.

Raisky OY, Wang WB, Alfano RR, et al. 1998. In1-xGaxAs1-yPay/InP multiple quantum well solar cell structures. J Appl Phys 84:5790–5794.

Schapers T, Engels G, Lange J, et al. 1998. Effect of the heterointerface on the spin splitting in modulation doped InxGa1-xAs/InP quantum wells for B -> O. J Appl Phys 83:4324–4333.

Taguchi K, Miyaji H, Izumi K, et al. 2002. Crystal growth of isotactic polystyrene in ultrathin films: film thickness dependence. J Macromol Sci Part B4 1:1033–1042.

Wells RL, Aubuchon SR, Kher SS, Lube MS, White PS. 1995. Synthesis of Nanocrystalline Indium Arsenide and Indium-Phosphide from Indium(Iii) Halides and Tris(Trimethylsilyl) Pnicogens—synthesis, characterization, and decomposition behavior of I3in-Center-Dot-P(Sime(3))(3). Chem Mater 7:793–800.

Zhuang QD, Yoon SF, Zheng HQ. 2000. Effect of matrix on InAs self-organized nanostructures on InP substrate. Commad 2000 Proc 455–458.